Journal of Medicinal Chemistry

ARTICLE

pubs.acs.org/jmc

Bisphosphonamidate Clodronate Prodrug Exhibits Potent Anticancer Activity in Non-Small-Cell Lung Cancer Cells

Marie R. Webster,[†] Ming Zhao,[‡] Michelle A. Rudek,[‡] Christine L. Hann,[§] and Caren L. Freel Meyers*[,†]

[†]Department of Pharmacology and Molecular Sciences, Johns Hopkins University School of Medicine, 725 N. Wolfe Street, WBSB 305, Baltimore, Maryland 21201, United States

[‡]Analytical Pharmacology Core of the Sidney Kimmel Comprehensive Cancer Center at Johns Hopkins University School of Medicine, Baltimore, Maryland, United States

[§]Department of Oncology, Johns Hopkins University School of Medicine, Baltimore, Maryland, United States

Supporting Information

ABSTRACT:

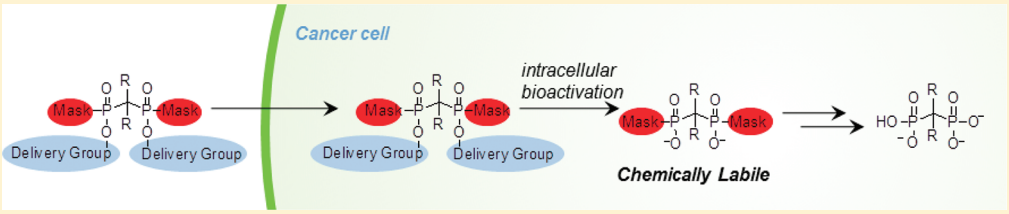

Bisphoshonates are used clinically to treat disorders of calcium metabolism, hypercalcemia and osteoporosis, and malignant bone disease. Although these agents are commonly used in cancer patients and have potential direct anticancer effects, their use for the treatment of extraskeletal disease is limited as a result of poor cellular uptake. We have designed and synthesized bisphosphonamidate prodrugs that undergo intracellular activation to release the corresponding bisphosphonate and require only two enzymatic activation events to unmask multiple negative charges. We demonstrate efficient bisphosphonamidate activation and significant enhancement in anticancer activity of two bisphosphonamidate prodrugs in vitro compared to the parent bisphosphonate. These data suggest a novel approach to optimizing the anticancer activities of commonly used bisphosphonates.

INTRODUCTION

Clinically used bisphosphonates (BPs) are stable analogues of naturally occurring pyrophosphate.[1,2] BPs are known to inhibit cancer cell adhesion and invasion and to inhibit the growth of cancer cells in the bone microenvironment.[3,4] The two bisphosphonate classes, nitrogen-containing (NBP) and non-nitrogen-containing (NNBP), are distinguished structurally by the substitution pattern at the bridging methylene of the P−C−P linkage (Figure 1). The NBP class incorporates a nitrogen-containing substituent at the bridging methylene (e.g., zoledronate, aledronate, pamidronate), whereas the NNBP class lacks this nitrogen-containing substituent (e.g., clodronate, etidronate).

These BP classes are further distinguished by differences in mechanism of action. The NBP class inhibits an essential enzyme in isoprenoid biosynthesis, farnesyl pyrophosphate synthase (FPPS), leading to lower FPP levels and subsequent reduction in downstream protein prenylation events in osteoclasts and malignant bone cells. Recent reports suggest that increased levels of the FPPS substrate IPP, caused by inhibition of FPPS by NBPs, promote formation of AppIPP (triphosphoric acid 1-adenosine-5′-yl ester 3-(3-methylbut-3-enyl) ester), which is believed to induce apoptosis.[5] In contrast, NNBPs undergo conversion to the corresponding nonhydrolyzable ATP analogues. Clodronate is

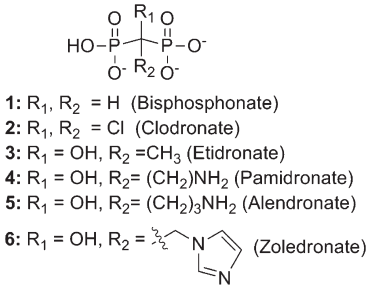

Figure 1. Structures of nitrogen-containing bisphosphonates (NBPs) and non-nitrogen-containing bisphosphonates (NNBPs).

metabolized to the ATP analogue AppCCl$_2$p (adenosine 5′-β-γ-dichloromethylene triphosphophosphate), which is believed to be the active metabolite responsible for the apoptotic activity of clodronate observed in osteoclasts and malignant bone cells.[6,7] Further, AppCCl$_2$p was shown to inhibit mitochondrial metabolism through inhibition of ADP/ATP translocase, and it is

Received: April 28, 2011
Published: August 24, 2011

Scheme 1. Proposed Intracellular Bioreductive Activation of Bisphosphonamidate Prodrugs (R = H or Cl)

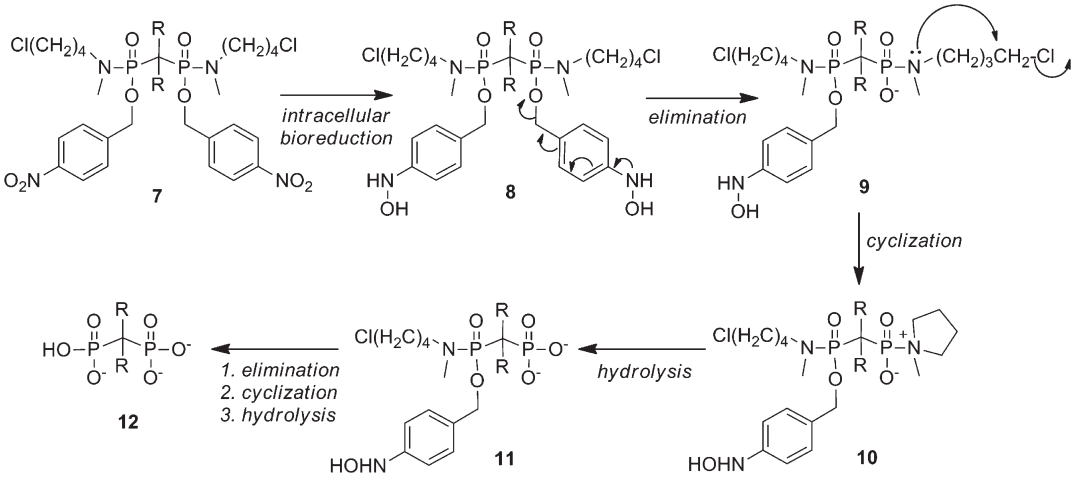

conceivable that additional targets are susceptible to inhibition by $AppCCl_2p$.[8]

Skeletal-related events (SKE) such as fracture, spinal cord compression, and hypercalcemia are common and cause significant morbidity in cancer patients with bone metastases.[9] Bisphosphonate therapy has been shown to reduce the rate of SKE in several clinical trials, leading to its use as a standard adjunct therapy in patients with bone metastases. The clinical success of NBPs in the prevention and management of bone metastatases has led to the evaluation of BPs as potential therapeutic agents for the treatment of cancer in soft tissues.[1] The NBP zoledronate (**6**, Figure 1) is a commonly used BP in metastatic bone disease and exhibits varying anticancer activities with IC_{50} ranging from 3 to >100 μM in several cancer cell lines.[1,10,11] The cytotoxic effects of zoledronate in cancer cells are believed to be exerted through a variety of mechanisms, including blockage of cell cycle in models of non-small-cell lung cancer,[12] inhibition of angiogenesis,[13−16] and induction of apoptosis in small-cell lung cancer cell lines,[11] although the molecular mechanisms beyond inhibition of FPPS are not well-understood.

NNBPs, including clodronate (**2**, Figure 1), are significantly less potent anticancer agents,[17] exhibiting growth inhibition in the high micromolar or low millimolar range in breast and ovarian cancers[10] and minimal activity against lung cancer cell lines.[10] The anticancer activity of clodronate is thought to correlate with formation of $AppCCl_2p$ in breast, prostate, and myeloma cells;[18] however, the molecular mechanisms underlying the anticancer effects of clodronate are not well-understood.

BPs are polyanionic at physiologic pH and are consequently concentrated in the mineralized bone matrix.[19] While beneficial for the treatment of bone disorders, this structural characteristic of BPs precludes efficient uptake into extraskeletal tumor cells. The low cellular uptake of BPs presents a critical barrier both for the development of these agents to treat tumors in soft tissues and for studies to elucidate the intracellular mechanisms by which BPs exert antitumor effects.

Existing strategies to increase bioavailability of NNBPs such as clodronate have involved masking of the BP scaffold with biodegradable or chemically labile groups designed to release the corresponding BP through nonspecific esterase activation or chemical hydrolysis postintestinal absorption.[20−22] These prodrugs generally undergo rapid extracellular bioactivation in serum, leading to partially unmasked, impermeable intermediates, which are often inefficiently converted to the fully unmasked BP.[20] There are no such prodrug strategies reported for BPs bearing the tertiary hydroxyl group at the bridging methylene position, including the NBP class, owing to the intrinsic instability of these compounds when masked as tetraesters.[23] Other strategies to increase BP cell permeability have focused on introducing modifications at the bridging methylene of the P−C−P linkage to increase hydrophobicity. Such modifications have also been shown to impart changes in target specificity.[24−26] Increasing hydrophobicity of substituents at the bridging methylene group does not overcome low membrane permeability entirely, as phosphonate masking strategies have been employed in these cases as well.[22,27]

Here we report a novel bisphosphonamidate prodrug strategy for the intracellular release of bisphosphonates and demonstrate its application to bisphosphonic acid and the clinically used NNBP clodronate. Our results suggest bisphosphonamidate prodrugs undergo rapid activation to release the corresponding BP following reductive activation of nitroaryl delivery groups. Further, we demonstrate intracellular conversion of a bisphosphonamidate prodrug to the corresponding bisphosphonate and a remarkable enhancement in anticancer activity of two bisphosphonamidate prodrugs compared to the parent bisphosphonates in A549 cells.

RESULTS

Design and Synthesis of Bisphosphonamidate Prodrugs. We have designed a prodrug strategy to enhance membrane permeability of bisphosphonates through incorporation of two biodegradable nitroaryl delivery groups and two halobutylamine masking groups, which effectively mask the polyanionic charges (Scheme 1). The bisphosphonate design shown here extends the halobutyl phosphoramidate prodrug strategy developed for the intracellular delivery of nucleotides.[28]

Membrane permeable bisphosphonamidate prodrugs (**7**) are designed to undergo rapid intracellular bioreduction to produce the corresponding hydroxylamine **8** (Scheme 1), which undergoes elimination through the aromatic ring and expulsion of phosphonamidate anion **9**. The resulting increase in electron density of the phosphonamide nitrogen atom facilitates a cyclization

Scheme 2. Synthesis of Prodrugs 14 and 15[a]

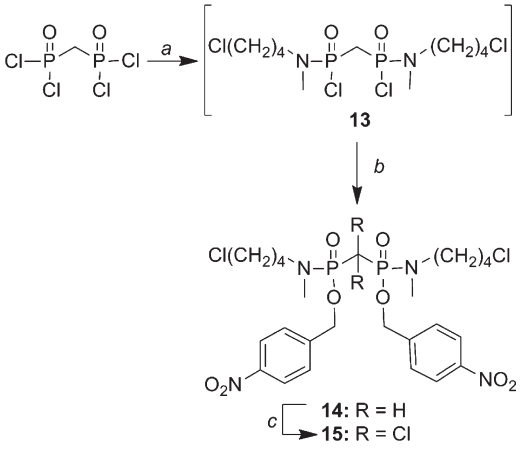

[a] Reaction conditions: (a) *N*-methyl-*N*-(4-chlorobutyl)amine hydrochloride, DIPEA, CH_2Cl_2, 0 °C; (b) nitrobenzyl alochol, DIPEA, DMAP, room temp; (c) NaOCl, benzyltriethyl ammonium chloride, CCl_4, MeOH.

reaction to produce the corresponding zwitterionic intermediate **10**. Subsequent rapid P−N bond hydrolysis affords the unmasked phosphonate **11** in a manner similar to nucleotide release.[28,29] The release of the second phosphonyl group is achieved in the same manner to give the fully unmasked bisphosphate **12**. Although it is difficult to predict the kinetics of activation, efficient release of the fully unmasked bisphosphonate is expected. An advantage of this strategy over existing bisphosphonate prodrug strategies is the requirement of a minimal number of enzymatic bioactivation steps to unmask multiple negative charges. As with the chemical deprotection of phosphoryl ester groups, removal of the first protective group is most often rapid while removal of the second masking group is considerably slower as a result of increased electron density at the phosphoryl leaving group and a slower rate of elimination.[30] The prodrug design incorporates a single nitroaryl delivery group at each phosphonyl group that is susceptible to rapid intracellular enzymatic activation by nitroreduction. The subsequent activation steps to release the fully unmasked bisphosphonate rely only upon the intrinsic chemical reactivity of the enzymatically reduced bisphosphonamidate **8** rather than subsequent, inefficient enzymatic activation events.

Bisphosphonamidate prodrugs were synthesized as diastereomeric mixtures (Scheme 2). Des-chloro bisphosphonamidate **14** was prepared via a two-step, one-pot synthesis. *N*-Methyl-*N*-chlorobutylamine hydrochloride was prepared as previously described.[31] Coupling of *N*-methyl-*N*-chlorobutylamine substituents to methylenebis(phosphonic dichloride) in the presence of DIPEA was monitored using ^{31}P NMR. In a representative synthesis, complete conversion to intermediate **13** was confirmed by the disappearance of the starting methylenebis(phosphonic dichloride) at δ −1.53 ppm (relative to TPPO) and appearance of two ^{31}P resonances at δ 6.17 and 6.10 ppm (1.7:1), indicating the formation of phosphonamidate dichloride **13** as a diastereomeric mixture. Treatment of **13** with nitrobenzyl alcohol in the presence of DIPEA and a nucleophilic catalyst (DMAP) afforded bisphosphonamidate prodrug **14** as a diastereomeric mixture (δ 0.84 and 0.81 ppm, 1.3:1), along with apparent hydrolysis product (~20%). Clodronate prodrug **15** was prepared by chlorination of

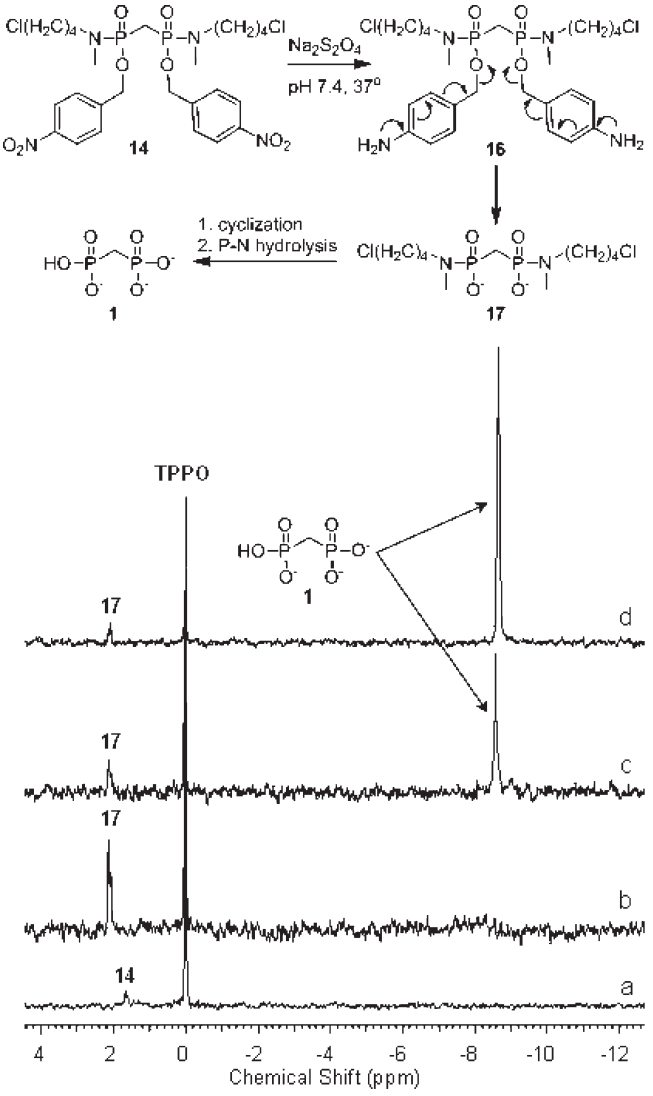

Figure 2. Reductive activation of BP prodrug **14**: (a) prodrug **14** prior to reduction; (b) following addition of dithionite to **14**; (c) at 4 h; (d) following addition of authentic **1** to reaction mixture shown in (c).

bisphosphonamidate **14**. In a representative synthesis, bisphosphonamidate **14** (1.5:1 mixture of diastereomers) was treated with sodium hypochlorite, resulting in a new set of ^{31}P resonances corresponding to a diaseteromeric mixture of clodronate prodrug **15** (−9.80 and −9.98 ppm, 1:1.6).

Confirmation of Bisphosphonamidate Activation. To confirm the release of a fully unmasked bisphosphonate following reduction of the bisphosphonamidate nitrobenzyl ester, bisphosphonamidate prodrug **14** was subjected to chemical reduction by dithionite under model physiologic conditions, and the subsequent reactions were monitored using ^{31}P NMR (Figure 2). Upon solubilization and reduction of **14**, a resonance appearing at +2 ppm (relative to TPPO) was observed in the ^{31}P NMR spectrum (Figure 2b). Conversion of this peak to a new resonance at −8.5 ppm (Figure 2c) was observed and is consistent with elimination and release of the bisphosphonate **1**. Confirmation of bisphosphonate release was accomplished by comparison to authentic bisphosphonate **1** (Figure 2d).

Inhibition of Cell Proliferation by Bisphosphonate Prodrugs. Clodronate has shown little or no antiproliferative effects

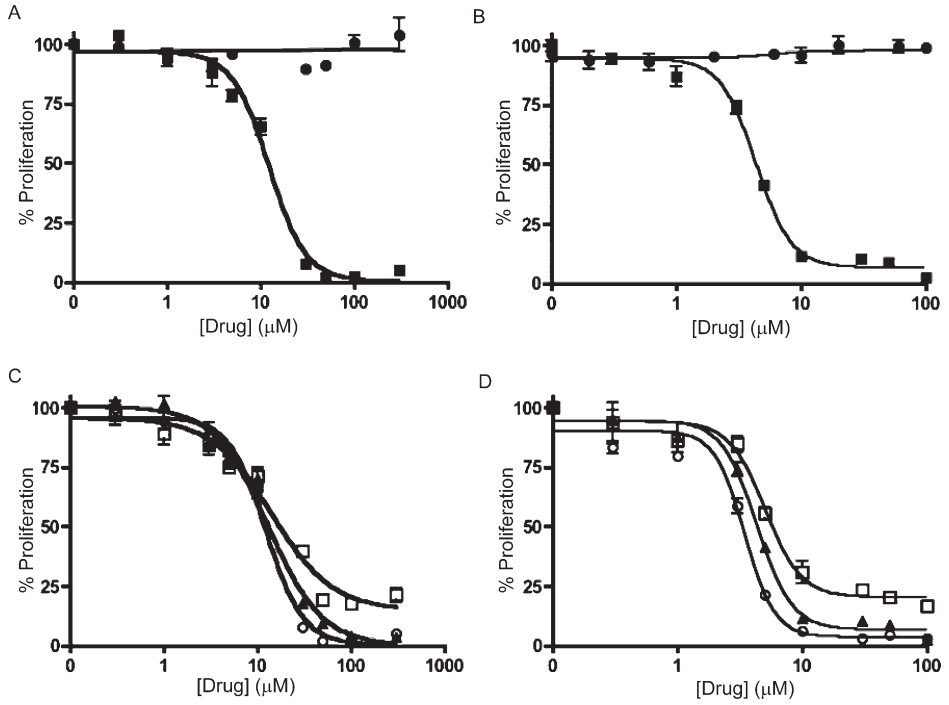

Figure 3. Effect of bisphosphonate prodrug **14** and clodronate prodrug **15** on proliferation of A549 cells, determined using the MTS assay. Results are displayed as % of control. (A) Bisphosphonate prodrug **14** (■) shows an enhanced antiproliferative effect compared to bisphosphate (●) at 72 h. (B) Clodronate prodrug **15** (■) shows an enhanced antiproliferative effect compared to clodronate (●). (C) Effect of **14** at 24 h (□), 48 h (▲), and 72 h (○). (D) Effect of **15** at 24 h (□), 48 h (▲), and 72 h (○).

Table 1. In Vitro Effects of 14 and 15 on A549 NSCLC Cells

	14		15	
time (h)	IC_{50} (μM)[a]	EC_{50} (μM)[b]	IC_{50} (μM)[a]	EC_{50} (μM)[b]
24	17 ± 4	nd[c]	7.6 ± 3	nd[c]
48	15 ± 0.4	24 ± 4	5.2 ± 1	19 ± 4
72	13 ± 1	25 ± 4	4.4 ± 2	16 ± 1

[a] IC_{50} is concentration of **14** or **15** that decreased cell proliferation by 50% compared to control. [b] EC_{50} is the concentration of **14** or **15** that decreased cell number by 50% compared to control. [c] The viability of A549 cells did not decrease by 50% after 24 h of treatment with **14** or **15**.

against multiple cells lines, in part because of low membrane permeability. Bisphosphonates **14** and **15** are fully masked and are expected to have increased cell permeability. As predicted, both **14** and **15** exhibit potent activity against A549 NSCLC cells in vitro (Figure 3) as determined by the MTS cell proliferation assay. Dose−response curves were generated using drug concentrations ranging from 0.2 to 300 μM, and cell proliferation was measured at 24, 48, and 72 h after drug treatment (Figure 3, Table 1). Consistent with published reports,[10] clodronate does not exhibit a detectable growth inhibitory effect at concentrations up to 1 mM against the growth of A549 cells. In contrast, clodronate prodrug **15** and bisphosphonate prodrug **14** exhibit remarkably enhanced activity with IC_{50} values of 4.4 ± 2 and 13 ± 1 μM, respectively, at 72 h (Figure 3A,B). While it is possible the diastereomers of **14** and **15** may be activated at different rates, they release the same achiral bisphosphonate, and comparable antiproliferative activities are observed with different diastereomeric mixtures (data not shown).

Permeability and Intracellular Activation of Prodrug 14. The enhanced activity of prodrugs **14** and **15** against A549 cells (Figure 3) is consistent with increased cell permeability of these analogues. To provide further evidence that bisphosphonamidates are cell permeable, intracellular levels of prodrug **14** were measured in A549 cells treated with prodrug at varying concentrations (0, 10, or 30 μM) for 8 h. As expected, LC−MS−MS analysis of cell lysate in each case indicates that reasonably high intracellular prodrug levels are achieved in a concentration-dependent manner, with 68.6 and 169.3 ng/10^4 cells **14** detected in cells treated with 10 and 30 μM **14**, respectively (Figure 4A).

Bisphosphonamidate **14** is designed to undergo intracellular activation to release the corresponding bisphosphonate **1**. Direct detection of intracellular bisphosphonate by mass spectrometry is difficult, as these highly polar compounds have low ionization efficiency. Thus, chemical derivatization of bisphosphonate released intracellularly was carried out in an effort to provide evidence for intracellular prodrug activation. *N-tert*-Butyldimethylsilyl-*N*-methyltrifluoroacetamide (MTBSTFA) has been used successfully to derivatize polar functional groups, including carboxylic acids, for mass spectrometry analysis.[32,33] MTBSTFA has also been used as a derivatizing agent for the detection of phosphonate-bearing 2-(phosphonomethyl)pentanedioic acid (2-PMPA).[34] Thus, we have used MTBSTFA as derivatization agent for the qualitative detection of **1** released from prodrug **14** intracellularly. The presence of intracellular bisphosphonate **1** in A549 cells treated for 8 h with prodrug **14** (10 or 30 μM) or bisphosphonate **1** (30 μM) was confirmed by detection of the corresponding tetrasilylated derivative **18** formed following treatment of cell lysate with MTBSTFA. Indeed, tetrasilyl bisphosphonate **18** was detected in A549 cells treated with

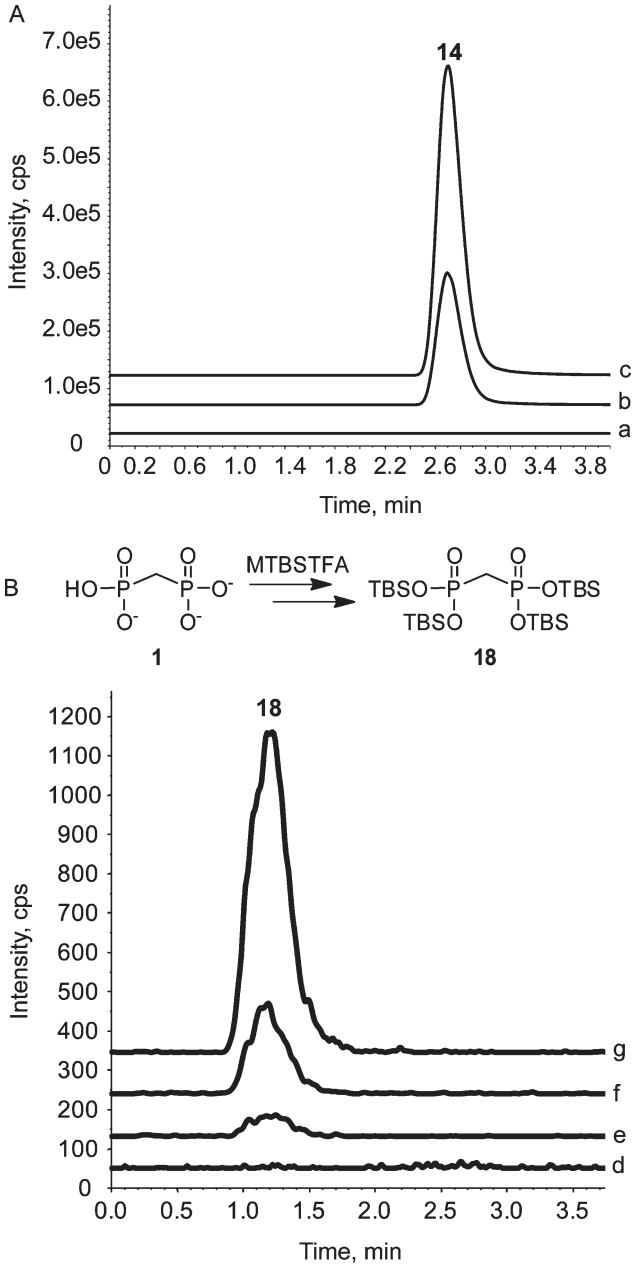

Figure 4. Prodrug **14** is cell permeable (A) and undergoes intracellular activation in A549 cells to release bisphosphonate **1** (B). (A) Ion chromatograms showing absence of prodrug **14** in untreated cells (a) and detection of **14** (68.6 ng/10^4 cells) in cells treated with 10 μM **14** (b) and cells treated with 30 μM **14** (169.3 ng/10^4 cells) (c). (B) Ion chromatograms showing absence of tetrasilyl bisphosphonate **18** following MTBSTFA reaction of lysate from untreated cells (d) and detection of **18** in cells treated with 30 μM bisphosphonate **1** (e), cells treated with 10 μM prodrug **14** (f), and cells treated with 30 μM prodrug **14** (g). Ion chromatograms are offset in the *y*-dimension for clarity.

bisphosphonamidate **14** and at considerably lower levels in cells treated with free bisphosphonate **1** at a comparable concentration (Figure 4B).

Cell Viability. In order to correlate the growth inhibitory effects of **14** and **15** with cell viability, absolute cell number at varying drug concentration was determined using a trypan blue exclusion assay. The number of viable cells at each dose was

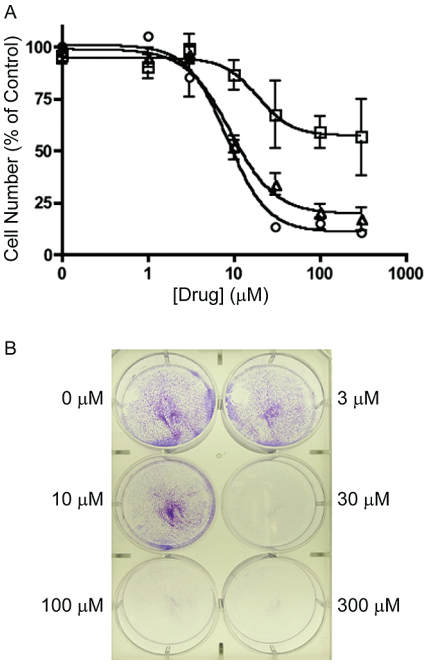

Figure 5. Effect of **15** on cell viability of NSCLC cells. Cell number was determined using trypan blue. (A) Decrease in number of NSCLC cells by **15** at 24 (□), 48 (▲), 72 (○) h. (B) Crystal violet staining of A549 NSCLC cells treated with **15** for 72 h.

determined at 0, 24, 48, and 72 h following drug treatment and plotted as a percent of control (Figure 5A). The EC_{50} of **15** determined at 48 h is 19 ± 4 μM, ~3.6-fold higher than its IC_{50} determined by the MTS assay (Table 1). A similar difference in the effects of **15** on cell viability versus inhibition of proliferation was observed after a 72 h drug treatment. Interestingly, at 24 h, cell viability was reduced by only 57% at the highest drug concentration tested; therefore, an EC_{50} was not determined. In parallel, viable cells were stained with crystal violet at 72 h following drug treatment to further demonstrate the marked reduction in cell viability upon treatment with clodronate prodrug **15** (Figure 5B). In order to confirm this reduction in cell viability, cells treated with **15** for 72 h (at 10, 30, 100, and 300 μM) were washed to remove the prodrug and fresh medium without drug was added. Cells were then allowed to grow for an additional 48 h. No new cell growth was observed in wells containing cells treated with **15** (data not shown). Prodrug **14** affects cell viability in a similar manner with an EC_{50} at 48 h that is ~1.6-fold greater than its IC_{50} determined using the MTS assay.

Cell Cycle. PI and flow cytometry analysis were performed to study the effects of prodrug **15** on cell cycle. Cell cycle analysis of cells treated with 0, 3, 10, or 30 μM **15** for 72 h suggested cell cycle arrest with low micromolar concentrations of **15**. Unequivocal support of G_1 cell cycle arrest was obtained through flow cytometry analysis of cells treated with 0, 3, or 10 μM **15** for 72 h and with nocodazole treatment for the last 24 h of prodrug exposure. Nocodazole is a microtubulin polymerization inhibitor, known to cause G_2 cell cycle arrest. In the absence of prodrug **15**, nocadazole-induced G_2 arrest is evident (Figure 6B). However, in the presence of prodrug, a marked accumulation of cells in G_1 is observed as low as 3 μM, indicating G_1 cell cycle arrest caused by prodrug **15**.

dx.doi.org/10.1021/jm200521a |*J. Med. Chem.* 2011, 54, 6647–6656

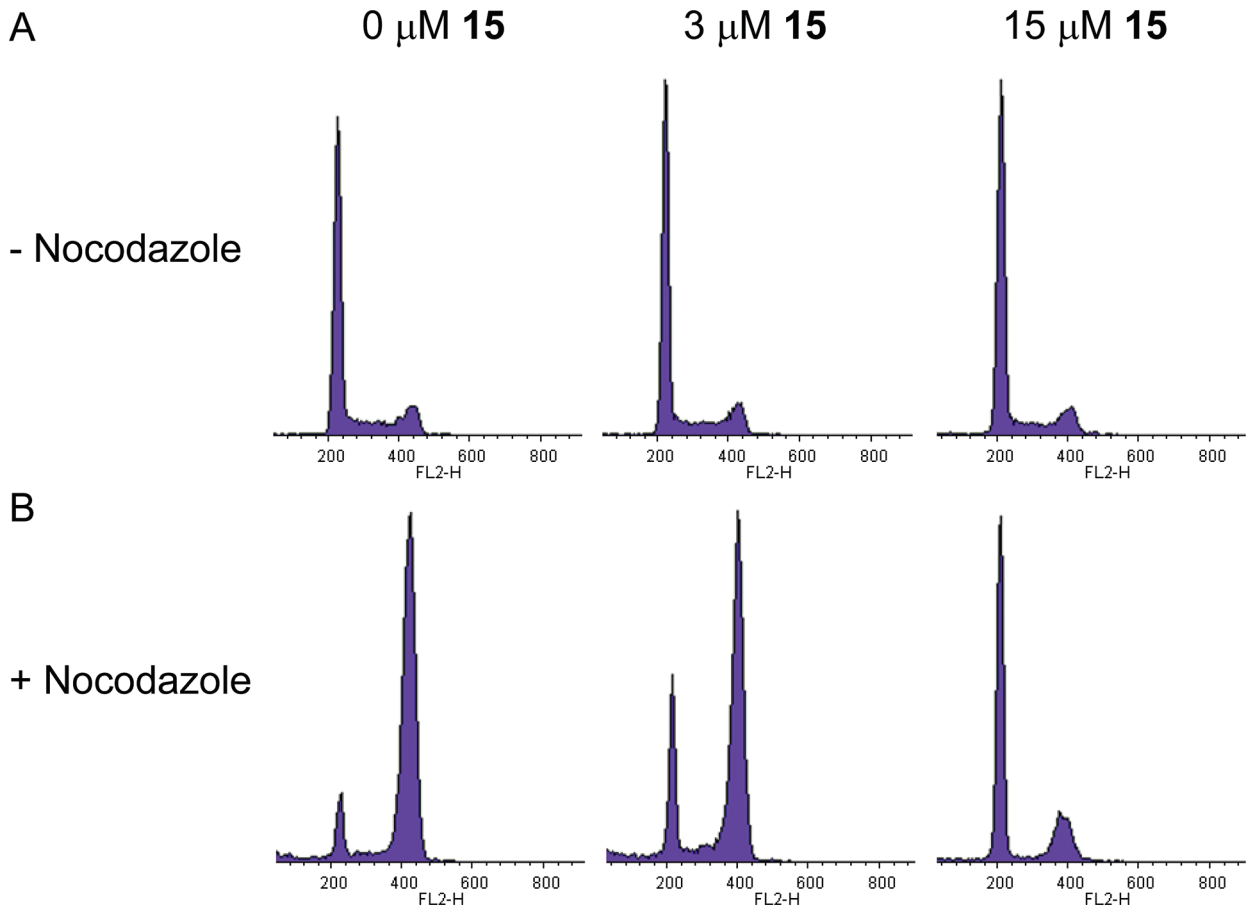

Figure 6. Effect of clodronate prodrug **15** on cell cycle, determined using the PI and FACS analysis. (A) A549 cells treated with 0, 3, and 10 μM **15** for 72 h. (B) A549 cells treated with 0, 3, and 10 μM **15** for 72 h and nocodazole for the final 24 h. In the nocodazole-treated cells, accumulation of cells in the G_1 phase is evident at 3 and 10 μM **15**.

DISCUSSION AND CONCLUSIONS

The poor cellular uptake of bisphosphonates into soft tissues has limited their use in the treatment of extraskeletal diseases and detailed studies to elucidate the molecular mechanisms underlying the anticancer activity of this compound class. We sought to develop a more efficient strategy for the intracellular delivery of bisphosphonates in order to realize the potential of this clinically used compound class for the treatment of extraskeletal tumors. The bisphosphonamidate prodrugs described here are designed to be more membrane permeable than the corresponding free bisphosphonates and undergo efficient bioreductive activation to release either bisphosphonate or clodronate intracellularly. A bisphosphonamidate prodrug was rapidly activated to the corresponding bisphosphonate under model physiological conditions following chemical reduction of the nitroaryl delivery groups. Formation of free bisphosphonate as the only product is consistent with an activation mechanism that takes place via elimination, cyclization, and P−N bond hydrolysis (Figure 2). As no other bisphosphonate ester intermediates were observed in the ^{31}P NMR spectrum, P−N bond hydrolysis prior to C−O cleavage is an unlikely activation pathway.

In this study, clodronate and bisphosphonate exhibited minimal activity against A549 cells up to 1 mM. The bisphosphonamidate prodrugs described here exhibit >250-fold increase in growth inhibitory activity against A549 cells, compared to the free bisphosphonates. This remarkable enhancement in potency is presumably due to increased cell permeability of the prodrug, which allows for a substantial increase in intracellular bisphosphonate concentration. The LC−MS−MS detection of reasonably high intracellular prodrug concentrations and the observation that bisphosphonate is released intracellularly support this idea. However, cytotoxicity of the prodrug itself cannot be ruled out as a contributing factor in the observed activity of these prodrugs. A partial growth inhibitory effect of the clodronate prodrug on A549 cells is observed as early as 24 h, and complete growth inhibition by the prodrug is observed by 48 and 72 h. The observed partial growth inhibitory effect at 24 h may reflect the dependence upon prodrug activation to release the corresponding bisphosphonate, the conversion of bisphosphonate to its active metabolite (AppCH$_2$p or AppCCl$_2$p), and subsequent action of these metabolites on cellular target(s). T4 RNA ligase has been shown to effectively convert NNBPs to their ATP analogues.[35] Both bisphosphonate and clodronate are known to be substrates of T4 RNA ligase with clodronate being converted to AppCCl$_2$p more efficiently than the corresponding conversion of the nonchlorinated bisphosphonate to AppCH$_2$p. On this basis, we anticipate that intracellular conversion of bisphosphonate to AppCH$_2$p is also less efficient than the conversion of clodronate to AppCCl$_2$p. The observed 3-fold decrease in IC_{50} of **14** compared to **15** is consistent with this idea. Detailed studies to determine the kinetics of intracellular prodrug activation and clodronate metabolism are required to correlate these events with observed growth in inhibitory activity.

To provide further evidence for the anticancer activity of bisphosphonamidate prodrugs **14** and **15**, a complementary assay was performed to evaluate the effects of the bisphosphonamidate prodrugs on cell viability. Cell number was determined at each dose at 24, 48, and 72 h. Interestingly, **15** decreases the viability of A549 cells to just above 50% of control at higher doses over 24 h. However, a more pronounced effect on cell proliferation was observed at 24 h in the MTS assay. The difference between antiproliferative activity and effects on cell viability at 24 h suggests that **14** and **15** exert effects on metabolic activity, which leads to cell death over time. Taken together with the observation that somewhat higher prodrug concentrations are required for effects on cell viability, these results are consistent with a mechanism of action involving prodrug activation to the corresponding bisphosphonate and subsequent conversion to the nonhydrolyzable ATP analogue.

The more potent clodronate prodrug **15** was selected for cell cycle analysis studies. PI and flow cytometry analysis of A549 cells treated with the clodronate prodrug over 72 h suggested G_1 cell cycle arrest of A549 cells at low concentrations of prodrug **15**. G_1 cell cycle arrest was unequivocally confirmed in nocodazole-treated cells where an obvious shift from nocodazole-induced G_2 arrest to G_1 arrest occurred in the low micromolar range of prodrug **15**. G_1 cell cycle arrest correlates with the antiproliferative activity of this compound, suggesting that prodrug **15** affects mitochondrial function, which leads to cell cycle arrest and eventually cell death.

The low membrane permeability of bisphosphonates imposes a significant barrier to the development of these agents for the treatment of extraskeletal tumors. Clodronate displays varying effects in different cancer cell types,[10] with minimal activity against lung cancer cells. Studies to investigate differences in the mechanism of clodronate action that could account for these differences are also impeded by poor cellular uptake. We have developed a bisphosphoamidate prodrug strategy that significantly enhances the membrane permeability of bisphosphonates through incorporation of two biodegradable nitroaryl delivery groups and two halobutyl amine masking groups. The use of only two biodegradable delivery groups takes advantage of the most efficient enzymatic activation steps and exploits the exquisite reactivity of chemically labile halobutyl phosphonamidate anion intermediates along the prodrug activation pathway for rapid intracellular activation and release of the fully unmasked bisphosphonate. The remarkable enhancement of activity of bisphosphonamidate prodrugs in A549 cells compared to the parent BPs highlights the potential utility of this approach to extend the use of bisphosphonates beyond the treatment of skeletal diseases and presents a potential tool for investigating bisphosphonate mechanism of action.

EXPERIMENTAL PROCEDURES

All ^{31}P and ^{1}H NMR spectra were acquired on a 400 MHz Varian or Brüker NMR. ^{31}P shifts were recorded in parts per million and referenced to triphenylphosphine oxide (TPPO) as the coaxial reference in either benzene or benzene-d_6. ^{1}H chemical shifts are reported in parts per million from tetramethylsilane. HMRS characterization of prodrugs was carried out at the University of Illinois Mass Spectrometry Lab using ES ionization. All reactions were carried out under argon unless otherwise noted. Methylene chloride and diisopropylethylamine were obtained from commercial sources and distilled prior to use. A549 cells were maintained in 1640 RMPI with 10% FBS, 1% pen/strep, 1% glutamate, and 1% sodium pyruvate. *N*-Methyl-*N*-(4-chlorobutyl)amine hydrochloride was synthesized as previously described.[31] Methylenediphosphonic acid, dichloromethylenediphosphonic acid disodium salt, and nocodazole used in biological assays were obtained from commercial sources. Methylenediphosphonic acid was determined to be >95% pure by sodium hydroxide titration, determined by vendor. Dichloromethylenediphosphonic acid was submitted, by the vendor, to elemental analysis: calculated C (4.95%), found C (4.2%); the amount of water was determined to be 2% by the Karl Fischer method. Nocodazole was determined to be ≥95% pure by reverse-phase HPLC. LC−MS−MS experiments were conducted using an AB Sciex triple quadrapole TM 5500 mass spectrometric detector (Applied Biosystems, Foster City, CA, U.S.). The instrument was equipped with an electrospray interface in positive ion mode and controlled by the Analyst, version 1.2, software (Applied Biosystems).

4-Nitrobenzyl Methylenebis(*N*-4-chlorobutyl-*N*-methylphosphonamidate) 14. Methylenebis(phosphonic dichloride) (0.466 g, 1.87 mmol) and *N*-methyl-*N*-(4-chlorobutyl)amine hydrochloride (0.589 g, 3.73 mmol) were dissolved in CH_2Cl_2 (7.48 mL) and cooled to 0 °C with stirring under an Ar atmosphere. DIPEA (1.56 mL, 8.98 mmol) was added dropwise. The reaction mixture was allowed to warm to room temperature, and stirring was continued for 2 h. Nitrobenzyl alcohol (1.43 g, 9.35 mmol) was added to the reaction mixture in one portion. In a separate flask under an Ar atmosphere, DMAP (0.228 mg, 1.87 mmol) was dissolved in CH_2Cl_2 (0.2 mL) and DIPEA (0.782 mL, 4.49 mmol), and the resulting mixture was added dropwise to the reaction mixture at room temperature. The reaction mixture was stirred at room temperature for 4 h. ^{31}P NMR analysis of the crude reaction mixture showed a 1.3:1 diastereomeric mixture. The mixture was washed with saturated NH_4Cl (1 × 2 mL). The organic layers were combined, dried over $NaSO_4$, and concentrated under reduced pressure. Removal of impurities by flash chromatography (1:99, MeOH/ethyl acetate) resulted in the isolation of a 1.9:1 diastereomeric mixture of **14** as a pale yellow oil, in 32% yield. The purity of **14** was determined to be >95% by HPLC (C_{18} Rocket column). The method was as follows: 100% water to 100% acetonitrile over 3 min, then 5 min at 100% acetonitrile; retention time was 3.3 min. ^{31}P NMR ($CDCl_3$) δ 1.00 and 0.88 ppm (1.9:1 mixture); ^{1}H NMR ($CDCl_3$) δ 8.23 and 8.19 (d, 4H, 1:1.9 mixture); 7.61 and 7.54 (d, 4H, 1:1.9 mixture); 5.21 and 5.19 (m, 4H, 1:1.9 mixture); 4.94 (m, 2H); 3.56 (m, 4H); 3.25 and 3.15 (m, 2H, 1.9:1 mixture); 2.97 (m, 2H); 2.68 and 2.65 (d, 6H, 1.9:1 mixture); 2.51 and 2.41 (t, 2H, diastereotopic), 1.73 (m, 8H). HRMS: calcd for $C_{25}H_{37}N_4O_8P_2Cl_2$, m/z 653.1464 $[M + H]^+$; found, 653.1467.

4-Nitrobenzyl Dichloromethylenebis(*N*-4-chlorobutyl-*N*-methylphosphonamidate) 15. Bisphosphonamidate **14** (0.350 g, 0.536 mmol) was dissolved in CCl_4 (1.2 mL) and MeOH (0.6 mL). Benzyltriethylammonium chloride (0.054 g, 0.236 mmol) was added in one portion. Then 10% NaOCl solution (1.8 mL) was added with stirring. The reaction was monitored by ^{31}P NMR over 4 h until completion. ^{31}P NMR analysis of the crude reaction mixture showed a 1:1.6 diastereomeric mixture of **15**. The reaction mixture was quenched with saturated NH_4Cl solution (2 mL), and the product was extracted using CH_2Cl_2 (2 × 0.5 mL). Removal of impurities by flash chromatography (100% ethyl acetate to 5:95 MeOH/ethyl acetate) resulted in the isolation of a 1:1 diastereomeric mixture of **15** as a pale yellow oil, in 60% yield. Purity of **15** was determined to be >95% by HPLC (Altima C_{18} column, 250 mm × 4.6 mm i.d.). Method was as follows: 5:95 water/acetonitrile to 75% acetonitrile over 5 min, 75% acetonitrile for 5 min, 75−100% acetonitrile over 5 min, then 100% acetonitrile for 5 min; retention time was 15.2 min. Although a diastereomeric mixture of **15** was observed by ^{31}P NMR during reaction monitoring in methylene chloride as the reaction solvent, the diastereomers of purified **15** appear identical by ^{31}P NMR in $CDCl_3$. ^{31}P NMR ($CDCl_3$) δ −9.46 (s); ^{1}H NMR ($CDCl_3$) δ 8.25 and 8.21 (d, 4H, 1:1 mixture); 7.65 and 7.62 (d, 4H, 1:1 mixture); 5.41 (m, 2H); 5.26 (m, 2H); 3.53 (m, 4H); 3.42 (m, 2H); 3.13 (m, 2H); 2.90 and 2.86

(d, 6H, 1:1 mixture); 1.72(m, 8H). HRMS: calcd for $C_{25}H_{35}N_4O_8P_2Cl_4$, *m/z* 721.0684 $[M + H]^+$; found, 721.0682.

^{31}P NMR Detection of Prodrug Activation. A suspension of BP prodrug **14** (22 mM) was prepared with sonication in a 1:2:8 mixture of DMF/acetonitrile/cacodylate buffer (200 mM, pH 7.4) at 37 °C, and the ^{31}P chemical shift was recorded. Under these conditions, **14** appeared as a single resonance, and low signal intensity was observed as a result of low solubility of the prodrug under these conditions. After addition of dithionite (8 molar equiv), signal intensity increased as a consequence of increased solubility of reduced and/or eliminated species. The reaction mixture was incubated at 37 °C for the duration of the experiment.

In Vitro Cell Proliferation Assays. Cell proliferation was determined using the CellTiter 96 Aqueous One Solution Cell Proliferation Assay MTS assay. A549 NSCLC cells were plated at 1.5×10^3 cells per well in flat bottom 96-well plates in 99 μL of medium and allowed to adhere overnight. The drugs were serially diluted in 100% DMSO. For each drug treatment group, 1 μL of a 100× stock solution was added to each well for a final DMSO concentration of 1%. Cells were treated for 24, 48, or 72 h. Cells were incubated with MTS dye (20 μL well^{-1}) for 40 min to 2 h. Absorbance at 490 nm was determined using a SpectraMax M2 (Molecular Devices) plate reader. The percent cell proliferation was calculated by converting the experimental absorbance to percentage of control, which was then plotted vs drug concentration. The IC_{50} values were determined using a nonlinear dose−response analysis in GraphPad Prism, version 4.0. The IC_{50} is defined as the concentration of drug needed to cause a 50% decrease in proliferation compared to vehicle control.

Detection of Intracellular Prodrug and Bisphosphonate. A549 NSCLC cells were plated at 1.3×10^5 cells per well in flat bottom six-well plates. Cells were dosed as described above. At 8 h following drug treatment, the medium was removed, and the cells were washed with 1 mL of PBS. Each well was trypsanized with 600 μL of trypsin for 3−5 min. The trypsin reaction was quenched with an equal volume of medium. The cells were transferred to a 15 mL conical and centrifuged at 1100 rpm for 5 min. Supernatant was removed, and the cells were resuspended in 200 μL of medium. The cells were diluted 1:1 in 0.04% trypan blue and counted using a cytometer. The number of cells was determined at each drug concentration and time. The cells were then centrifuged at 1100 rpm for 5 min. The supernatant was removed, and the cell pellets were washed 2× with PBS. The supernatant was removed, and the pellets were frozen at −80 °C until analysis.

For detection of bisphosphonamidate prodrug **14** in A549 cells treated for 8 h, the cell pellet was suspended in 0.5 mL of deionized water, and 100 μL of the suspension was lysed using 300 μL of acetonitrile containing temazepam (100 ng/mL) as an internal standard. The suspension was mixed vigorously for 1 min on a vortex mixer and then subjected to centrifugation at 1200*g* for 10 min at ambient temperature. The supernatant (10 μL) was injected into the LC−MS−MS instrument using an autosampling device operating at room temperature. Separation was achieved on a Waters X-Terra C_{18} (50 mm × 2.1 mm i.d., 3 μm) at room temperature using isocratic elution with acetonitrile/water mobile phase (60:40, v/v) containing 0.1% formic acid at a flow rate of 0.2 mL/min. Prodrug detection was performed using electrospray tandem mass spectrometry operating in positive ion mode by monitoring the ion transitions from *m/z* 653.0 → 532.0 (BP prodrug) and *m/z* 301.2 → 255.1 (temazepam). Samples were quantitated over the assay range of 2−1000 ng/mL. Samples were then quantitated in ng/10^4 cells as [nominal concentration (ng/mL)][5 (standardized dilution)]/[total number of cells (expressed as 10^4)].

For qualitative detection of intracellular bisphosphonate **1** in A549 cells treated for 8 h with prodrug **14** or bisphosphonate **1**, the cell pellet suspension was prepared as described above. Cell lysis was achieved by addition of 300 μL of acetonitrile to 100 μL of the cell suspension and 1000 ng/mL 2-(phosphonomethyl)pentanedioic acid (2-PMPA) as an internal standard. The suspension was mixed vigorously for 1 min on a vortex mixer and then subjected to centrifugation at 1200*g* for 10 min at ambient temperature. A volume of 300 μL of the supernatant was transferred to a glass test tube and evaporated to dryness under nitrogen at 40 °C. Acetonitrile (100 μL) was added to the residue along with 100 μL of *N-tert*-butyldimethylsilyl-*N*-methyltrifluoroacetamide (MTBSTFA). The mixture was subjected to vortex-mixing prior to and every 15 min during a 1 h incubation at 80 °C. After 1 h, the solution was cooled to room temperature and diluted in acetonitrile (1:5, v/v) prior to injection (10 μL) into the LC−MS−MS instrument using an autosampling device operating at room temperature. Separation was achieved on a Waters X-Terra C_{18} (50 mm × 2.1 mm i.d., 3 μm) at room temperature using isocratic elution with acetonitrile/water mobile phase (70:30, v/v) containing 0.1% formic acid at a flow rate of 0.2 mL/min. Detection of tetrasilyl bisphosphonate **18** was performed using electrospray tandem mass spectrometry operating in positive ion mode by monitoring the ion transitions from *m/z* 633.4 to 617.0 (derivatized bisphosphonate **18**) and from *m/z* 683.0 to 551.4 (derivatized 2-PMPA).

Cell Cycle Analysis. Cell cycle distribution was determined using flow cytometry. A549 NSCLC cells were plated at 6.7×10^4 cells per well in flat bottom six-well plates. Cells were dosed as described above. At 24, 48, or 72 h following drug treatment, the medium was collected and the cells were washed with 1 mL of PBS. Each well was trypsanized with 600 μL of trypsin for 3−5 min. The trypsin reaction was quenched with an equal volume of medium. All supernatants and washes were combined and centrifuged at 1500 rpm for 5 min. Supernantant was decanted, and the cells were washed with 2 mL of 1% FBS/PBS. Cells were centrifuged at 1500 rpm for 5 min, and the supernantant was decanted. Cells were resuspended in 1 mL of cold PBS, fixed in 9 mL of cold 70% ethanol, and incubated at 4 °C for at least 30 min. Cells were centrifuged at 1500 rpm for 5 min, washed with 1% FBS/PBS, and resuspended in 1 mL of 2:1 1% FBS in PBS/phosphate citric acid buffer (pH 7.8). Cells were incubated at room temperature for 5 min, then spun at 1500 rpm for 5 min. The supernatant was decanted, and the cells were resuspended and incubated in 300 μL of PBS/FBS/PI/RNase solution (10 μg/mL propidium iodide and 3 KU of RNase A) for 30 min at 37 °C. Flow cytometry was performed to analyze DNA content, collecting 10 000 PI positive gated events per sample.

In Vitro Cell Count. A549 NSCLC cells were plated at 1.7×10^4 cells per well in flat bottom 12-well plates. Cells were dosed as described above. At 24, 48, or 72 h following drug treatment, the medium was collected, and the cells were washed with 200 μL of PBS. Each well was trypsinized with 200 μL of trypsin for 3−5 min. The trypsin reaction was quenched with an equal volume of medium. All supernatants and washes were combined and spun at 1500 rpm for 5 min. Supernatant was decanted, and the cells were resuspended in 200 μL of medium. The cells were diluted 1:1 in 0.04% trypan blue and counted using a cytometer. The absolute number of cells was determined at each drug concentration. The cell number for each concentration was converted to percent of control for each time point and plotted using GraphPad Prism 4.0. The EC_{50} was calculated as the concentration of drug that caused a 50% decrease in number of cells compared to control.

Crystal Violet Assay. A549 NSCLC cells were plated at 1.7×10^4 cells per well in flat bottom six-well plates. Cells were dosed as described above. Cells were analyzed at 24, 48, and 72 h. The medium was removed, and the cells were washed twice with PBS. The cells were then stained with crystal violet solution (1 mL well^{-1}, 0.5% crystal violet in 95% EtOH) for 5−15 min. The stain was removed, and the plates were rinsed with cold water and dried at room temperature.

■ ASSOCIATED CONTENT

Ⓢ Supporting Information. Characterization data for **14** and **15**, including NMR and HPLC results; stability of **14** and **15**

in media; control experiment assessing chemical conversion of prodrug **14** to derivatized bisphosphonate **18**. This material is available free of charge via the Internet at http://pubs.acs.org.

AUTHOR INFORMATION

Corresponding Author
*Phone: 410-502-4807. Fax: 410-955-3023. E-mail: cmeyers@jhmi.edu.

DISCLOSURE

The contents of the studies are solely the responsibility of the authors and do not necessarily represent the official view of NCRR or NIH.

ACKNOWLEDGMENT

This research was supported by the Flight Attendants Medical Research Institution (FAMRI) Center for Excellence at the Johns Hopkins University School of Medicine. Mass spectrometry studies were supported by the Analytical Pharmacology Core of the Sidney Kimmel Comprehensive Cancer Center at Johns Hopkins (NIH Grants P30 CA006973 and UL1 RR025005 and the Shared Instrument Grant 1S10RR026824-01). Mass spectrometry studies were supported in part by Grant UL1 RR 025005 from the National Center for Research Resources (NCRR), a component of the National Institutes of Health (NIH) and NIH Roadmap for Medical Research. We thank Dr. Charles Rudin and Dr. Richard Borch for critical evaluation of the manuscript. We also thank Dr. Timothy Burns for his contribution to the design and analysis of flow cytometery experiments.

ABBREVIATIONS USED

BP, bisphosphonates; NBP, nitrogen-containing bisphosphonates; NNBP, non-nitrogen-containing bisphosphonates; SCLC, small-cell lung cancer; NSCLC, non-small-cell lung cancer; FPP, farnesyl pyrosphosphate; FPPS, farnesyl pyrophosphate synthase; SKE, skeletal related events

REFERENCES

(1) Morgan, G.; Lipton, A. Antitumor Effects and Anticancer Applications of Bisphosphonates. *Semin. Oncol.* **2010**, *37* (5), S30–S40.

(2) Gnant, M. Bisphosphonates in the Prevention of Disease Rcurrence: Current Results and Ongoing Trials. *Curr. Cancer Drug Targets* **2009**, *9*, 824–833.

(3) Boissier, S.; Magnetto, S.; Frappart, L.; Cuzin, B.; Ebetino, F. H.; Delmas, P. D.; Clezardin, P. Bisphosphonates Inhibit Prostate and Breast Carcinoma Cell Adhesion to Unmineralized and Mineralized Bone Extracellular Matrices. *Cancer Res.* **1997**, *57* (18), 3890–3894.

(4) Boissier, S.; Ferreras, M.; Peyruchaud, O.; Magnetto, S.; Ebetino, F. H.; Colombel, M.; Delmas, P.; Delaissé, J. M.; Clézardin, P. Bisphosphonates Inhibit Breast and Prostate Carcinoma Cell Invasion, an Early Event in the Formation of Bone Metastases. *Cancer Res.* **2000**, *60* (11), 2949–2954.

(5) Räikkönen, J.; Taskinen, M.; Dunford, J. E.; Mönkkönen, H.; Auriola, S.; Mönkkönen, J. Correlation between Time-Dependent Inhibition of Human Farnesyl Pyrophosphate Synthase and Blockade of Mevalonate Pathway by Nitrogen-Containing Bisphosphonates in Cultured Cells. *Biochem. Biophys. Res. Commun.* **2011**, *407*, 663–667.

(6) Rogers, M. J.; Ji, X. H.; Russell, R. G. G.; Blackburn, G. M.; Williamson, M. P.; Bayless, A. V.; Ebetino, F. H.; Watts, D. J. Incorporation of Bisphosphonates into Adenine-Nucleotides by Amebas of the Cellular Slime-Mold *Dictyostelium discoideum*. *Biochem. J.* **1994**, *303*, 303–311.

(7) Frith, J. C.; Monkkonen, J.; Blackburn, G. M.; Russell, R. G. G.; Rogers, M. J. Clodronate and Liposome-Encapsulated Clodronate Are Metabolized to a Toxic ATP Analog, Adenosine 5′-(beta,gamma-dichloromethylene)Triphosphate, by Mammalian Cells in Vitro. *J. Bone Miner. Res.* **1997**, *12* (9), 1358–1367.

(8) Lehenkari, P. P.; Kellinsalmi, M.; Napankangas, J. P.; Ylitalo, K. V.; Monkkonen, J.; Rogers, M. J.; Azhayev, A.; Väänänen, K. Further Insight into Mechanism of Action of Clodronate: Inhibition of Mitochondrial ADP/ATP Translocase by a Nonhydrolyzable, Adenine-Containing Metabolite. *Mol. Pharmacol.* **2002**, *62*, 1255–1262.

(9) Domcheck, S. M.; Younger, J.; Finkelstein, D. M.; Seiden, M. V. Predictors of Skeletal Complications in Patients with Metastic Breast Carcinoma. *Cancer* **2000**, *89*, 363–368.

(10) Knight, L. A.; Conroy, M; Fernando, A.; Polak, M.; Kurbacher, C. M.; Cree, I. A. Pilot Studies of the Effect of Zoledronic Acid (Zometa) on Tumor-Derived Cells ex Vivo in the ATP-Based Tumor Chemosensitivity Assay. *Anti-Cancer Drugs* **2005**, *16* (9), 969–976.

(11) Matsumoto, S.; Kimura, S.; Segawa, H.; Kuroda, J.; Yuasa, T.; Sato, K.; Nogawa, M.; Tanaka, F.; Maekawa, T.; Wada, H. Efficacy of the Third-Generation Bisphosphonate Zoledronic Acid Alone and Combined with Anti-Cancer Agents against Small Cell Lung Cancer Cell Lines. *Lung Cancer* **2005**, *47* (1), 31–39.

(12) Li, Y.; Chang, J. W.; Chou, W. C.; Liaw, C. C.; Wang, H. M.; Huang, J. S.; Wang, C. H.; Yeh, K. Y. Zoledronic Acid Is Unable to Induce Apoptosis, but Slows Tumor Growth and Prolongs Survival for Non-Small-Cell Lung Cancers. *Lung Cancer* **2008**, *59* (2), 180–191.

(13) Wood, J.; Bonjean, K.; Ruetz, S.; Bellahcene, A.; Devy, L.; Foidart, J. M.; Castronovo, V.; Gree, J. R. Novel Antiangiogenic Effects of the Bisphosphonate Compound Zoledronic Acid. *J. Pharmacol. Exp. Ther.* **2002**, *302* (3), 1055–1061.

(14) Croucher, P. I.; De Raeve, H.; Perry, M. J.; Hijzen, A.; Shipman, C. M.; Lippitt, J.; Green, J.; Van Marck, E.; Van Camp, B.; Venderkerken, K. Zoledronic Acid Treatment of 5T2MM-Bearing Mice Inhibits the Development of Myeloma Bone Disease: Evidence for Decreased Osteolysis, Tumor Burden and Angiogenesis, and Increased Survival. *J. Bone Miner. Res.* **2003**, *18* (3), 482–492.

(15) Santini, D.; Vincenzi, B.; Galluzzo, S.; Battistoni, F.; Rocci, L.; Venditti, O.; Schiavon, G.; Angeletti, S.; Uzzalli, F.; Caraglia, M.; Dicuonzo, G.; Tonini, G. Repeated Intermittent Low-Dose Therapy with Zoledronic Acid Induces an Early, Sustained, and Long-Lasting Decrease of Peripheral Vascular Endothelial Growth Factor Levels in Cancer Patients. *Clin. Cancer Res.* **2007**, *13* (15), 4482–4486.

(16) Hamma-Kourbali, Y.; Di Benedetto, M.; Ledoux, D.; Oudar, O.; Leroux, Y.; Lecouvey, M.; Kraemer, M. A Novel Non-Containing-Nitrogen Bisphosphonate Inhibits Both in Vitro and in Vivo Angiogenesis. *Biochem. Biophys. Res. Commun.* **2003**, *310* (3), 816–823.

(17) Lipton, A. Emerging Role of Bisphosphonates in the Clinic—Antitumor Activity and Prevention of Metatasis to Bone. *Cancer Treat. Rev.* **2008**, *34*, 525–530.

(18) Mönkkönen, H.; Kuokkanen, J.; Holen, I.; Evans, A.; Lefley, D. V.; Jauhiainen, M.; Auriola, S.; Mönkkönen, J. Bisphosphonate-Induced ATP Analog Formation and Its Effect on Inhibition of Cancer Cell Growth. *Anti-Cancer Drugs* **2008**, *19* (4), 391–399.

(19) Russell, R. G. G.; Watts, N. B.; Ebetino, F. H.; Rogers, M. J. Mechanisms of Action of Bisphosphonates: Similarities and Differences and Their Potential Influence on Clinical Efficacy. *Osteoporosis Int.* **2008**, *19* (6), 733–759.

(20) Ahlmark, M.; Vepsalainen, J.; Taipale, H.; Niemi, R.; Jarvinen, T. Bisphosphonate Prodrugs: Synthesis and in Vitro Evaluation of Novel Clodronic Acid Dianhydrides as Bioreversible Prodrugs of Clodronate. *J. Med. Chem.* **1999**, *42* (8), 1473–1476.

(21) Vepsalainen, J. Bisphosphonate Prodrugs. *Curr. Med. Chem.* **2002**, *9*, 1201–1208.

(22) Zhang, Y.; Leon, A.; Song, Y.; Studer, D.; Haase, C.; Koscielski, L. A.; Oldfield, E. Activity of Nitrogen-Containing and Non-Nitrogen Containing Bisphosphonates on Tumor Cell Lines. *J. Med. Chem.* **2006**, *49* (9), 5804–5814.

(23) Neimi, R.; Turhanen, P.; Vepsalainen, J.; Taipale, H.; Jarvinen, T. Bisphosphonate Prodrugs: Synthesis and in Vitro Evaluation of Alkyl and Acyloxymethyl Esters of Etidronic Acid as Bioreversible Prodrugs of Etidronate. *Eur. J. Pharm. Sci.* **2000**, *11* (2), 173–180.

(24) Szabo, C. M.; Matsumura, Y.; Fukura, S.; Martin, M. B.; Sanders, J. M.; Sengupta, S.; Cieslak, J. A.; Loftus, T. C.; Lea, C. R.; Lee, H. J.; Koohang, A.; Coates, R. M.; Sagami, H.; Oldfield, E. Inhibition of Geranylgeranyl Diphosphate Synthase by Bisphosphonates and Diphosphates: A Potential Route to New Bone Antiresorption and Antiparasitic Agents. *J. Med. Chem.* **2002**, *45* (11), 2185–2196.

(25) Shull, L. W.; Wiemer, A. J.; Hohl, R. J.; Wiemer, D. F. Synthesis and Biological Activity of Isoprenoid Bisphosphonates. *Bioorg. Med. Chem.* **2006**, *14* (12), 4130–4136.

(26) Barney, R. J.; Wasko, B. M.; Dudakovic, A.; Hohl, R. J.; Wiemer, D. F. Synthesis and Biological Evaluation of a Series of Aromatic Bisphosphopnates. *Bioorg. Med. Chem.* **2010**, *18* (20), 7212–7220.

(27) Wiemer, A. J.; Yu, J. S.; Shull, W. L.; Barney, R. J.; Wasko, B. M.; Lamb, K. M.; Hohl, R. J.; Wiemer, D. F. Pivaloyloxymethyl-Modified Isoprenoid Bisphosphonates Display Enhanced Inhibition of Cellular Geranylgeranylation. *Bioorg. Med. Chem.* **2008**, *16* (7), 3652–3660.

(28) Tobais, S. C.; Borch, R. F. Synthesis and Biological Studies of Novel Nucleoside Phosphoramidate Prodrugs. *J. Med. Chem.* **2001**, *44* (25), 4475–4480.

(29) Tobias, S. C.; Borch, R. F. Synthesis and Biological Evaluation of a Cytarabine Phosphoramidate Prodrug. *Mol. Pharmaceutics* **2004**, *1* (2), 112–116.

(30) Cox, J. R.; Ramsay, O. B. Mechanisms of Nucleophilic Substitution in Phosphate Esters. *Chem. Rev.* **1964**, *64* (4), 317–352.

(31) Meyers, C. L.; Borch, R. F. A Novel Method for the Preparation of Nucleoside Diphosphates. *Org. Lett.* **2001**, *3* (23), 3765–3768.

(32) Prieto, J. A.; Andrade, F.; Martin, S.; Sanjuro, P.; Elorz, J.; Aldámix-Eschevarría, L. Determination of Creatine and Guanidinoacetate by GC−MS study of Their Stability in Urine at Different Temperatures. *Clin. Biochem.* **2009**, *42*, 125–128.

(33) Wood, P. L.; Khan, M. A.; Moskai, J. R. Neurochemical Analysis of Amino Acids, Polyamines and Carboxylic Acids: GC−MS Quantitation of *t*BDMS Derivatives Using Ammonia Positive Chemical Ionization. *J. Chromatogr., B* **2006**, *831*, 313–319.

(34) Yang, W.; Laws, K. A.; Sleczka, B.; S. Burak, E. S. (Guilford Pharmaceuticals, Inc., Baltimore, MD 21224). Development of a LC/MS/MS Method for the Quantitation of 2-(Phosphonomethyl)pentanedioic Acid in Rat Plasma and Brain. Presented at the 1998 American Association of Pharmaceutical Scientists (AAPS) Annual Meeting, 1998; Abstract 2397.

(35) Sillero, M. A. G.; Diego, A.; Silles, E.; Perez-Zuniga, F.; Sillero, A. Synthesis of Bisphosphonate Derivatives of ATP by T4 RNA Ligase. *FEBS Lett.* **2006**, *580* (24), 5723–5727.